Proc. Natl. Acad. Sci. USA
Vol. 84, pp. 7009–7013, October 1987
Biochemistry

Binding of a reduced peptide inhibitor to the aspartic proteinase from *Rhizopus chinensis*: Implications for a mechanism of action

(x-ray crystallography/rhizopuspepsin/substrate binding/catalysis)

K. SUGUNA*, EDUARDO A. PADLAN*, CLARK W. SMITH†, WILLIAM D. CARLSON‡, AND DAVID R. DAVIES*

*Laboratory of Molecular Biology, National Institute of Diabetes and Digestive and Kidney Diseases, National Institutes of Health, Bethesda, MD 20892; †Biopolymer Chemistry Unit, The Upjohn Company, Kalamazoo, MI 49001; and ‡Cardiac Unit, Massachusetts General Hospital, Boston, MA 02114

Contributed by David R. Davies, June 11, 1987

ABSTRACT **A peptide inhibitor, having the sequence D-His-Pro-Phe-His-PheΨ[CH_2-NH]Phe-Val-Tyr, with a reduced bond between the two adjacent phenylalanines, has been diffused into crystals of the aspartic proteinase from *Rhizopus chinensis* (rhizopuspepsin, EC 3.4.23.6). X-ray diffraction data to 1.8-Å resolution have been collected on the complex, which has been subjected to restrained least-squares refinement to an *R*-factor ($R = \Sigma||F_o| - |F_c||/\Sigma|F_o|$, where $|F_o|$ and $|F_c|$ are the observed and calculated structure factor amplitudes, respectively) of 14.7%. The inhibitor lies within the major groove of the enzyme and is clearly defined with the exception of the amino-terminal D-histidine and the carboxyl-terminal tyrosine. The reduced peptide bond is located in the active site with close contacts to the two catalytic aspartyl groups. The active-site water molecule that is held between the two carboxyl groups is displaced by the inhibitor, as are a number of other water molecules seen in the binding groove of the native enzyme. A mechanism of action for this class of enzymes is proposed from these results.**

The aspartic proteinases, which include the mammalian enzymes pepsin, gastricsin, chymosin, cathepsin D, and renin, as well as a number of microbial and plant enzymes, form a class of digestive enzymes having several common properties. They are optimally active at acidic pH, have two aspartic acids at the active site, and are all inactivated by certain inhibitors, such as pepstatin. In addition, they all display subsite specificities extending for several residues on either side of the scissile bond. Detailed x-ray analyses for four of these enzymes—namely, pepsin and three fungal enzymes, penicillopepsin, endothiapepsin and rhizopuspepsin [refs. 1, 2 (pp. 137–150), 3–8] have shown very similar three-dimensional structures; this similarity is particularly evident in the enzyme active sites.

The mechanism of action of these proteinases has been extensively discussed (for review, see ref. 2). Earlier studies provided no compelling evidence for the formation of a covalent intermediate during catalysis (9, 10). Consequently, recent mechanistic hypotheses based on the three-dimensional structures of these enzymes have invoked nucleophilic attack by a water molecule on the carbonyl carbon, with possible intervention of the carboxyl groups of the enzyme in transferring a proton to the substrate amino group [refs. 2 (pp. 189–195), 11, 12]. However, the identity of this water molecule remains unresolved.

We describe an 1.8-Å analysis of the complex of rhizopuspepsin with a reduced peptide inhibitor of the sequence D-His-Pro-Phe-His-PheΨ[CH_2-NH]Phe-Val-Tyr [nomenclature of Spatola (13)] and relate these results to a mechanism of action for aspartic proteinases.

The publication costs of this article were defrayed in part by page charge payment. This article must therefore be hereby marked "*advertisement*" in accordance with 18 U.S.C. §1734 solely to indicate this fact.

MATERIALS AND METHODS

Crystals of the native enzyme were grown as described (8). The crystals belong to the space group $P2_12_12_1$ with $a = 60.31$ Å, $b = 60.60$ Å, and $c = 106.97$ Å (8). The complex was prepared by soaking each native crystal in a solution containing 10 μl of the mother liquor (1.5 mg of protein dissolved in 220 μl of the crystallization buffer) and 2 μl of inhibitor solution prepared by dissolving 0.5 mg of the inhibitor in 10 μl of methanol. Cell dimensions of the complex are as follows: $a = 60.37$ Å, $b = 60.61$ Å, and $c = 106.77$ Å.

Intensity data were collected using the Mark II multiwire area detector system at the University of California at San Diego [Resource for Protein Crystallography, National Institutes of Health Grant RR-01644 (14)] with two detectors. Using two crystals, a total of 118,370 reflections were collected to >1.8-Å resolution. Lorentz, polarization, and absorption corrections (15) were applied to the data, and the different frames were scaled together, which resulted in an average merging R_{sym} of 0.045 for 36,590 unique reflections, where $R_{sym} = \Sigma|\bar{I} - I|/\Sigma|I|$.

The *R*-factor ($\Sigma||F_1| - |F_2||/\Sigma|F_1|$) between this data set and the native data set (also to 1.8 Å) is 0.15. An electron density map, calculated using $|F_{complex}| - |F_{native}|$ as amplitudes and the phases of the native enzyme (8), clearly showed six of the eight residues of the inhibitor (the other two being D-His of the amino terminus and Tyr of the carboxyl terminus). A model was fitted to this density using the interactive molecular graphics program FRODO (16, 17) on an Evans and Sutherland (Salt Lake City) PS300 picture system.

The structure has been refined using the restrained least-squares program PROLSQ developed by Hendrickson and Konnert (18), which was modified (19) to make use of Agarwal's (20) fast-Fourier-transform algorithm for structure factor calculations. The starting model consisted of the native enzyme refined at 1.8-Å resolution (8) and the model of the inhibitor fitted to the electron density. The native enzyme has 374 solvent molecules; those in the binding region and those with high *B*-values (> 40 $Å^2$) and low occupancies (< 0.6) were excluded from the initial model of the complex. The "flap," a β-hairpin loop between residue-77 and residue-83 that projects over the binding cleft, showed some movement in the preliminary examination of the complex. Therefore the starting model of the protein was adjusted for six residues (76 to 81) in this region to account for the movement. Special bond distances and angle distances were incorporated into the program PROTIN (18) to account for the geometry at the reduced bond of the inhibitor—i.e., the tetrahedral configuration of the C and N atoms of the reduced peptide link. The *R*-factor after 20 cycles of refinement is 14.7%. The final model contains 344 water molecules. The refined set of coordinates has been deposited in the Protein Data Bank (21).

Abbreviations: $|F_o|$ and $|F_c|$, observed and calculated structure factor amplitude, respectively; S, subsite.

RESULTS

Fig. 1 shows the $2|F_o| - |F_c|$ map for the inhibitor region of the structure. The middle six residues are clearly visible and can be located with precision. The peptide is in an approximate extended conformation, having ϕ and φ values shown in Table 1. The reduced peptide link between P_1 and P_1' α carbons is twisted from planarity by 51°. The protein subsites S_4–S_2' that interact with the inhibitor side chains are defined in Table 2.

The inhibitor backbone forms a number of hydrogen bonds: Pro-2I§ *N·O* Water-876 (2.52 Å), Pro-2I *N·O* Water-877 (3.01 Å), Phe-3I *N·O*$^{\gamma 1}$ Thr-222 (2.90 Å), Phe-3I *O·N* Thr-222 (2.96 Å), Phe-3I *O·O* Water-578 (2.92 Å), His-4I *N·O*$^{\delta 1}$ Asp-79 (2.98 Å), His-4I *O·N* Gly-78 (3.18 Å), His-4I *N*$^{\varepsilon 2}$*·O* Water-578 (3.28 Å), Phe-5I *N·O* Gly-220 (2.90 Å), Phe-6I *N·O*$^{\delta 2}$ Asp-218 (2.83 Å), Phe-6I *O·N* Gly-78 (2.83 Å), Val-7I *N·O* Gly-37 (2.96 Å), Val-7I *O·N*$^{\varepsilon 1}$ Trp-194 (3.23 Å), Val-7I *O·O* Water-874 (2.60 Å). Every main-chain nitrogen and oxygen atom of the inhibitor from Phe-3I (P_3) to Val-7I (P_2') is hydrogen bonded with the surrounding protein atoms (Fig. 2). These include three hydrogen bonds with the "flap" region. A similar mode of binding with some of the same hydrogen bonds has been reported [ref. 2 (pp. 467–478), 23] for various inhibitors bound to endothiapepsin. One hydrogen bond between the N atom of the scissile bond and O$^{\delta 2}$ of the active aspartate Asp-218 (2.83 Å) could have implications for the mechanism of action of the proteinase. A possible hydrogen bond is formed between this nitrogen atom and the carbonyl oxygen of the P_2 residue of the inhibitor (Fig. 2).

The side chains of the inhibitor are held in place in subsites along the sides of the active site cleft. Extensive van der Waals contacts occur between the inhibitor and various residues of the enzyme (Table 2). The S_1 and S_1' subsites on either side of the scissile bond seem to be extended subsites, each involving several amino acid side groups. Some residues of the flap, Tyr-77, Gly-78, Asp-79 and Ser-81, make van der Waals contacts with residues P_2, P_1, and P_1' of the inhibitor. The carbon atom that corresponds to the carbonyl of the scissile bond makes short contacts with the C$^{\gamma}$, O$^{\delta 1}$, and O$^{\delta 2}$ atoms of both active aspartates and is closer to Asp-35 than to Asp-218.

Several water molecules that bind in the groove in the native enzyme and the calcium ion (8) are displaced by the inhibitor. These waters include Water-507 near the pseudodyad axis between the two carboxyl groups, as well as Water-858, the water molecule assigned a nucleophilic role by James and Sielecki (12). This latter water molecule is displaced by the side chain of the P_1 residue and cannot exist in this location in the presence of bound substrate.

The active-site region in the complex is very similar to that in the native enzyme. One striking result is that the positions of the active aspartates are not changed when the inhibitor binds, despite displacement of the water molecules, probably because the active aspartates are held rigidly in position by the hydrogen-bonding network within the protein. However, the flap does move significantly when the inhibitor binds; similar movements have been observed when pepstatin and pepstatin-like inhibitors bind to rhizopuspepsin (11, ¶), penicillopepsin [ref. 2 (pp. 163–177)], and endothiapepsin (23). The rms (root-mean-square) shift of the 60 atoms of the flap region, between residues 74 and 82, is 0.62 Å. The movement of the flap enhances the binding of the inhibitor by making several good hydrogen bonds and van der Waals contacts between the inhibitor and the flap. Because of this binding, the flap, which was quite mobile in the native structure, is stabilized in the complex with considerably lower *B* values as shown in Fig. 3.

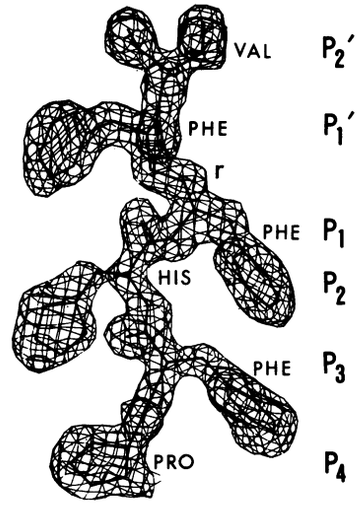

FIG. 1. $2|F_o| - |F_c|$ map showing the electron density of the inhibitor and fit of the model. r, Location of the reduced peptide bond.

The only other part of the protein that moves significantly is the side chain of Asn-119, a residue distant from direct contact with the inhibitor, being about 4.5 Å from Phe-5I. The movement of Asn-119 consists of a change of χ^1 from −49° to +59°; probable cause of this change is the displacement of a water molecule, Water-698, that hydrogen bonds to the sidegroup nitrogen in the native enzyme. The rearrangement of the Asn-119 side chain enables it to adopt a different hydrogen bonding interaction with Glu-16.

DISCUSSION

Most recent proposals for the mechanism of action of the aspartic proteinases have invoked a nucleophilic attack on the substrate carbonyl carbon by a water molecule, with general base catalysis by the aspartyl residues to protonate the amide nitrogen [refs. 2 (pp. 163–177), 4, 11, 24, 25]. The 2.1-Å analysis of endothiapepsin [refs. 2 (pp. 151–161), 26] led to a proposal in which the water molecule was held between the two active aspartic carboxyls as the nucleophile and a strain mechanism (27) was thought to distort the peptide group from its planar conformation, thus facilitating the formation of the tetrahedral intermediate [ref. 2 (pp. 189–195)]. Simultaneously, James and Sielecki [refs. 2 (pp. 163–177), 12] proposed a detailed mechanism, analyzed according to stereoelectronic principles, in which the nucleophile is not the water molecule located between the two

Table 1. Main-chain dihedral angles of the reduced peptide inhibitor

Residue	Angle, degree		
	ϕ	φ	ω
Pro-2I		163	179
Phe-3I	−114	158	180
His-4I	−140	65	180
Phe-5I	−99	59*	129*
Phe-6I	−84*	165	176
Val-7I	−113	152	

I, inhibitor.
*Reduced peptide link.

§Residues of the inhibitor are indicated by the letter I attached to the residue number.
¶Suguna, K., Davies, D. R. & Boger, J., American Crystallographic Association Annual Meeting, Aug. 18–25, 1985, Stanford, CA, p. 40 (abstr.).

Table 2. Contacts between rhizopuspepsin enzyme and the inhibitor

Inhibitor	Enzyme	Contacts, no.	Subsite*
Pro-2I	Thr-222	5	S_4
Phe-3I	Ile-15,Glu-16	6	S_3
	Thr-221		
His-4I	Gly-78,Asp-79	6	S_2
	Thr-221,Ile-225		
Phe-5I	Asp-33,Asp-35	23	S_1
	Tyr-77,Asp-79		
	Ser-81,Phe-114		
	Leu-122,Asp-218		
	Gly-220		
Phe-6I	Gly-37,Tyr-77	21	S_1'
	Gly-78,Ile-216		
	Asp-218,Trp-294		
	Ile-298		
Val-7I	Ser-38,Ile-75	9	S_2'
	Ser-76,Ile-130		
	Trp-194		

I, inhibitor.
*Notation of Schechter and Berger (22).

carboxyls, but another water molecule that forms a single hydrogen bond to the $O^{\delta 1}$ of Asp-35.

The observed displacement of water molecules from the active site upon inhibitor binding creates a problem when modeling the transition state with substrate. Assuming one of these waters is the nucleophile attacking the carbonyl carbon, this attack presumably occurs as the substrate is bound to the enzyme. In distinguishing between the conflicting hypotheses, the resulting model will naturally depend strongly on the assumptions used in designing the model. In particular, the outcome will depend on the position occupied by the carbonyl oxygen of the substrate in the Michaelis complex. Inhibitor studies suggest two possibilities. (*i*) For inhibitors of the pepstatin type, the hydroxyl group of the inhibitor occupies the central water position, and if this is also the position occupied by the oxygen of the substrate, then the attacking water will have to originate elsewhere. (*ii*) If, instead, the peptide bond is distorted by the optimal fitting of

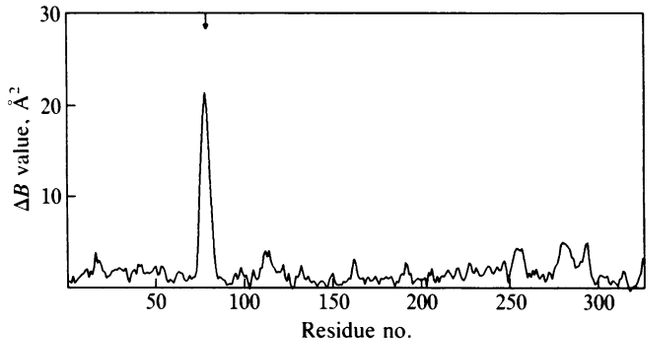

FIG. 3. A plot of the difference in the *B* values, indicative of thermal vibration of the α carbons of the free and bound structures of rhizopuspepsin versus the residue number. Arrow designates the flap region, site of considerable mobility reduction upon binding of the inhibitor.

the substrate into the cleft, as required by the inhibitor analysis described here, then the carbonyl oxygen will be displaced from the position of the central water, permitting the central water to be the attacking nucleophile. Because of the peculiar nature of the statyl residue (two additional atoms in the polypeptide backbone), we doubt that pepstatin can be used as a reliable model for the substrate–enzyme complex. Indeed, the P_2' side chain of pepstatin does not reside in S_2', but the backbone curls back to locate it in S_1' (11).

On the basis of these results, we propose a mechanism of action for rhizopuspepsin. First, consider the possible assignments of the protons. Fig. 4 shows the distances between the oxygen atoms of the catalytic site in the native enzyme in three different x-ray analyses. Allowing for errors in the structure determinations, these distances agree remarkably well and can be used to identify the hydrogen bonds and the possible locations of the protons. The pH rate profile for these enzymes (28) implies that in the active pH range the two carboxyls share one negative charge. The closer proximity of Water-507 to Asp-218 led us to assign this negative charge to Asp-218 (Fig. 5). It has generally been assumed that the lone proton resides between the two carboxyl oxygens, $O^{\delta 2}$ of Asp-35 and $O^{\delta 1}$ of Asp-218; based on geometrical consider-

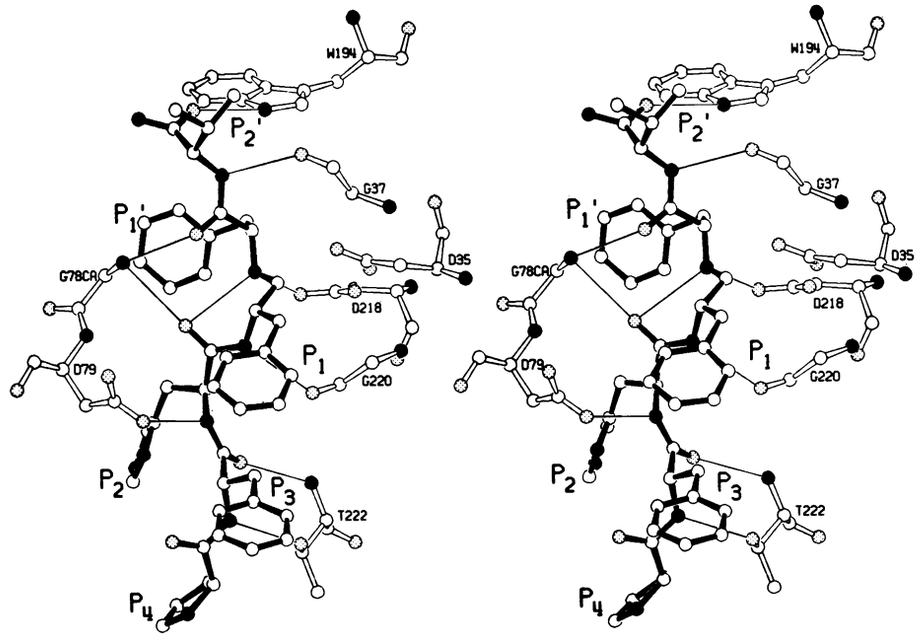

FIG. 2. Stereo drawing showing the hydrogen bonds between rhizopuspepsin and inhibitor (thick black lines). Residues are designated by one-letter amino acid nomenclature and sequence number.

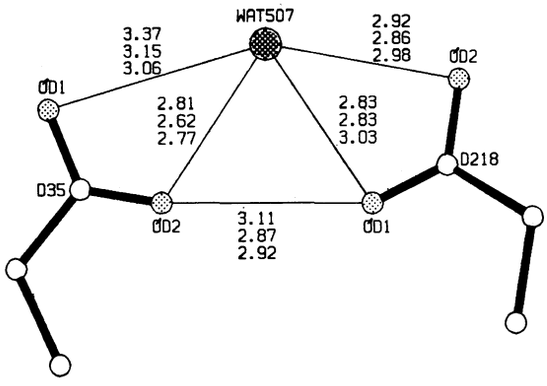

FIG. 4. Distances between the active aspartates and Water-507 (WAT507) in three different aspartic proteinases [refs. 2 (pp. 151–161), 4, 8]. D, Asp; OD1, $O^{\delta 1}$; OD2, $O^{\delta 2}$.

ations this is improbable. It has been noted (4, 8, 26) that these two oxygens are hydrogen bonded to the amide nitrogens of Gly-37 and Gly-220, respectively, thus restricting possible proton positions. Should we locate a proton on $O^{\delta 2}$ of Asp-35, unacceptable steric interactions would allow only one proton of Water-507 to hydrogen bond with the two carboxyls. However, should the proton be placed on $O^{\delta 1}$ of Asp-35, the water protons could lie in the general directions of $O^{\delta 2}$ of Asp-35 and $O^{\delta 2}$ of Asp-218. The symmetrical alternative could also occur. Experimental determination of the actual proton locations awaits neutron diffraction study.

The peptide inhibitor we studied cannot be an exact model for the tetrahedral intermediate because our inhibitor lacks the two oxygens on the reduced carbon atom. Also, the methylene group is within 1 Å of the position of Water-507 in the native structure and must be adjusted positionally to form an acceptable transition-state complex. Nevertheless, conformation of the studied peptide can indicate the kind of distortion to be expected upon binding of the substrate. To better understand stereochemical factors of the catalytic mechanism we have constructed a hypothetical model of substrate binding to rhizopuspepsin. As a first approximation, we conformed the backbone and side chains on either side of the scissile bond similarly to the conformations seen in this inhibitor, assuming preservation of the interactions between the enzyme and these atoms of the inhibitor when the substrate binds. This assumption is well supported by the network of specific hydrogen bonds to the backbone [on the N-terminal side of the inhibitor an identical hydrogen bond system is observed in pepstatin (11) and several pepstatin-like inhibitor complexes¶] and by the extensive interactions between the side chains and the enzyme. To adopt this conformation, rotation about the peptide bond must occur, causing the peptide group to depart from planarity. The direction and extent of this distortion have already been suggested by the deviation from planarity of the reduced peptide link in the inhibitor (see *Results*). This rotation reduces the double-bond character of the peptide bond and causes the nitrogen atom to move toward a pyramidal arrangement from the planar trigonal configuration of the undistorted peptide bond. This model was initially based on the reduced-peptide conformation and was then modified by making small adjustments needed to remove the close contact with Water-507. These adjustments were informed by knowledge of the refined structure of the rhizopuspepsin–pepstatin complex (11), where the hydroxyl group of the statyl residue occupies the water position.

In our model the carbonyl bond is oriented at ≈30° to the line between the carbonyl carbon and Water-507. Note that Water-507 can be displaced some distance from planarity with the carboxyl groups without breaking the system of hydrogen bonds. We anticipate that distortion of the peptide bond will be enhanced as a consequence of steric and

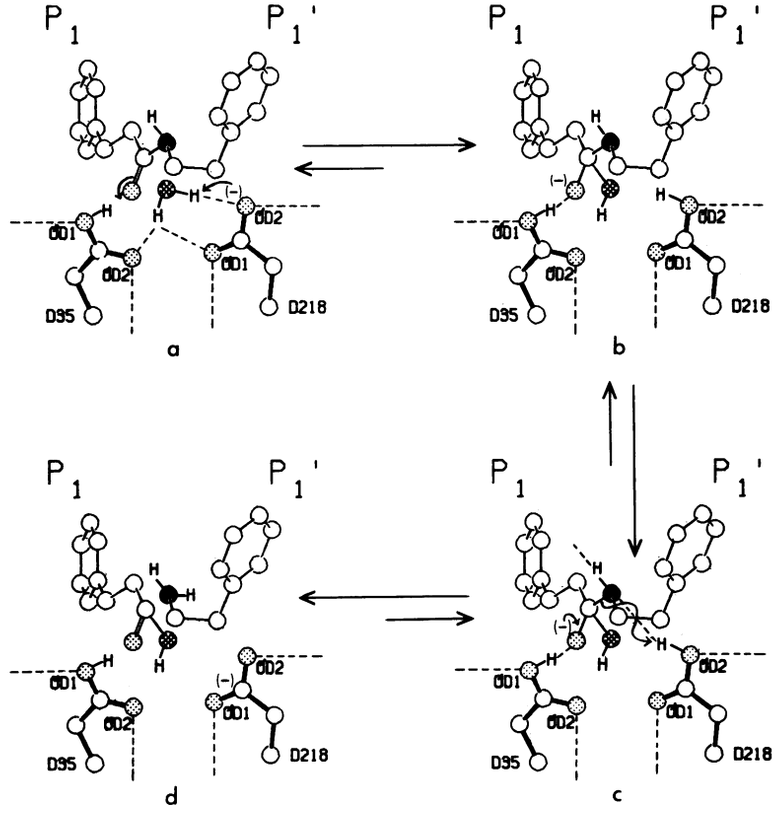

FIG. 5. The proposed catalytic mechanism for rhizopuspepsin (see text *Discussion*). D35, Asp-35; D218, Asp-218; OD1, $O^{\delta 1}$; OD2, $O^{\delta 2}$.

electrostatic repulsions between the carbonyl oxygen and this tightly bound water. Water-507 will now be in a position to engage in nucleophilic attack on the carbonyl carbon of the peptide bond; this water is made more nucleophilic by the system of hydrogen bonds to the carboxyl oxygens, facilitating transfer of a proton to Asp-218 (Fig. 5*b*). According to this model, the distortion from planarity positions the carbonyl oxygen of the scissile bond within hydrogen bonding distance of the $O^{\delta 1}$ of Asp-35 (Fig. 5), and also potentially with O^{γ} of Ser-38. The formation of a hydrogen bond between these atoms will further polarize the carbonyl bond, making the carbon atom more susceptible to nucleophilic attack. Of the two possible hydrogen positions on the pyramidal peptide nitrogen, one position points toward the carbonyl oxygen of the P_2 residue of the substrate. This weak hydrogen bond will localize the hydrogen in this position on the nitrogen, leaving the other direction free to accept a proton from the $O^{\delta 2}$ of Asp-218 (Fig. 5*c*). Rearrangement results in cleavage of the peptide bond (Fig. 5*d*), departure of the products, not necessarily simultaneously, and restoration of the active site to its original hydrated state.

Pearl (29) has recently proposed a detailed mechanism for aspartic proteinases in which the polarization of the carbonyl bond is achieved by forming hydrogen bonds with NH groups in the β-hairpin loop of the flap, specifically with the peptide NH groups of residues corresponding to Gly-78 and Asp-79 in rhizopuspepsin. Despite the apparent similarity in the mode of binding of reduced inhibitors to endothiapepsin [refs. 2 (pp. 467–478), 23] and the binding reported here, we have been unable to model the substrate-binding geometry proposed by Pearl. The extended conformation of the inhibitor seen in both cases makes it unlikely that the carbonyl oxygen interacts with the flap. Instead, we propose that the interaction with $O^{\delta 1}$ of Asp-35 and O^{γ} of Ser-38 can provide the polarizing environment of an oxyanion hole.

Close similarity of the known structures of aspartic proteinases suggests this mechanism might be valid for all members of this enzyme class. Our mechanism shares general features with the mechanism originally proposed by Pearl [ref. 2 (pp. 189–195)] that was based on the structure of endothiapepsin [refs. 2 (pp. 151–161), 26]. However, the higher resolution and greater degree in refinement of the structural complex we report and of the native rhizopuspepsin (8) enabled a more detailed correlation between structure and mechanism of action.

We thank Drs. Ben Dunn, Martin Karplus, Gerald Maggiora, and Attila Szabo for reading the manuscript and much useful advice. We particularly thank Dr. Dan Rich for many helpful comments, especially with regard to the mechanism proposed in Fig. 5.

1. Andreeva, N. S., Gustchina, A., Federov, A. A., Shutzkever, N. E. & Volnova, T. V. (1977) in *Acid Proteases, Structure, Function, and Biology*, ed. Tang, J. (Plenum. New York), pp. 23–31.
2. Kostka, V., ed. (1985) *Aspartic Proteinases and Their Inhibitors* (de Gruyter, Berlin).
3. Hsu, I.-N., Delbaere, L. T. J. & James, M. N. G. (1977) in *Acid Proteases, Structure, Function, and Biology*, ed. Tang, J. (Plenum, New York), pp. 61–81.
4. James, M. N. G. & Sielecki, A. R. (1983) *J. Mol. Biol.* **163,** 299–361.
5. Jenkins, J., Tickle, I., Sewell, T., Ungaretti, L., Wollmer, A. & Blundell, T. (1977) in *Acid Proteases, Structure, Function, and Biology*, ed. Tang, J. (Plenum, New York), pp. 43–60.
6. Subramanian, E., Liu, M., Swan, I. D. A. & Davies, D. R. (1977) in *Acid Proteases, Structure, Function, and Biology*, ed. Tang, J. (Plenum, New York), pp. 33–41.
7. Subramanian, E., Swan, I. D. A., Liu, M., Davies, D. R., Jenkins, J. A., Tickle, I. J. & Blundell, T. L. (1977) *Proc. Natl. Acad. Sci. USA* **74,** 556–559.
8. Suguna, K., Bott, R. R., Padlan, E. A., Subramanian, E., Sheriff, S., Cohen, G. H. & Davies, D. R. (1987) *J. Mol. Biol.*, in press.
9. Fruton, J. S. (1976) *Adv. Enzymol. Relat. Areas Mol. Biol.* **44,** 1–36.
10. Hofmann, T., Dunn, B. M. & Fink, A. L. (1984) *Biochemistry* **23,** 5247–5256.
11. Bott, R. R., Subramanian, E. & Davies, D. R. (1982) *Biochemistry* **21,** 6956–6962.
12. James, M. N. G. & Sielecki, A. R. (1985) *Biochemistry* **24,** 3701–3713.
13. Spatola, A. F. (1983) in *Chemistry and Biochemistry of Amino Acids, Peptides, and Proteins*, ed. Weinstein, B. (Dekker, New York), Vol. 7, pp. 267–357.
14. Xuong, Ng H., Freer, S., Hamlin, R., Nielsen, C. & Vernon, W. (1978) *Acta Crystallogr. Sect. A* **34,** 289–296.
15. Howard, A. J., Nielsen, C. & Xuong, Ng H. (1985) *Methods Enzymol.* **114,** 452–472.
16. Jones, T. A. (1978) *J. Appl. Crystallogr.* **11,** 268–272.
17. Pflugrath, J. W., Saper, M. A. & Quiocho, F. A. (1984) in *Methods and Applications in Crystallographic Computing*, eds. Hall, S. & Ashida, T. (Clarendon, Oxford), pp. 404–407.
18. Hendrickson, W. A. & Konnert, J. H. (1981) in *Biomolecular Structure, Conformation, Function and Evolution*, ed. Srinivasan, R. (Pergamon, Oxford), Vol. 1, pp. 43–57.
19. Finzel, B. C. (1987) *J. Appl. Crystallogr.* **20,** 53–55.
20. Agarwal, R. C. (1978) *Acta Crystallogr. Sect. A* **34,** 791–809.
21. Bernstein, F. C., Koetzel, T. F., Williams, G. J. B., Meyer, E. F., Jr., Brice, M. D., Rogers, J. R., Kennard, O., Shimanouchi, T. & Tasumi, M. (1977) *J. Mol. Biol.* **112,** 535–542.
22. Schechter, I. & Berger, A. (1967) *Biochem. Biophys. Res. Commun.* **27,** 157–162.
23. Foundling, S. I., Cooper, J., Watson, F. E., Cleasby, A., Pearl, L. H., Sibanda, B. L., Hemmings, A., Wood, S. P., Blundell, T. L., Valler, M. J., Norey, C. G., Kay, J., Boger, J., Dunn, B. M., Leckie, B. J., Jones, D. M., Atrash, B., Hallett, A. & Szelke, M. (1987) *Nature (London)* **327,** 349–352.
24. James, M. N. G., Hsu, I.-N. & Delbaere, L. T. J. (1977) *Nature (London)* **267,** 808–813.
25. James, M. N. G., Hsu, I.-N., Hofmann, T. & Sielecki, A. (1981) in *Structural Studies on Molecules of Biological Interest*, eds. Dodson, G., Glusker, J. P. & Sayre, D. (Clarendon, Oxford), pp. 350–389.
26. Pearl, L. & Blundell, T. (1984) *FEBS Lett.* **174,** 96–101.
27. Jencks, W. P. (1969) in *Catalysis in Chemistry and Enzymology* (McGraw-Hill, New York), pp. 294–308.
28. Hofmann, T., Hodges, R. S. & James, M. N. G. (1984) *Biochemistry* **23,** 635–643.
29. Pearl, L. (1987) *FEBS Lett.* **214,** 8–12.